Quasiparticle band structures of CuCl, CuBr, AgCl, and AgBr: The extreme case

Weiwei Gao, Weiyi Xia, Yabei Wu, Wei Ren, Xiang Gao, and Peihong Zhang

Quasiparticle Band Structures of CuCl, CuBr, AgCl, and AgBr: The Extreme Case

Weiwei Gao[1], Weiyi Xia[1], Yabei Wu[1,2], Wei Ren[2], Xiang Gao[3], and Peihong Zhang[1,2,3*]

[1]*Department of Physics, University at Buffalo, State University of New York, Buffalo, New York 14260, USA*

[2]*Department of Physics & International Center for Quantum and Molecular Structures, Shanghai University, Shanghai 200444, China*

[3]*Beijing Computational Science Research Center, Beijing 100084, China*

(Dated: June 21, 2018)

We present a systematic study of the quasiparticle band structures of transition metal halides CuCl, CuBr, AgCl, and AgBr. We show that GW calculations for cuprous halides are significantly more challenging computationally than ZnO, a much discussed *extreme* case. The local density approximation (LDA) within density functional theory severely underestimates the band gaps of CuCl and CuBr due to the inaccurate treatment of the semicore d electrons. As a result, many-body perturbation calculations within the G^0W^0 approach fails to give accurate quasiparticle properties starting from the LDA mean-field solution. The LDA+U method (with the screened Coulomb and exchange parameters calculated using a constrained random phase approximation approach), on the other hand, provides a much better starting point for subsequent G^0W^0 calculations. When properly converged, the G^0W^0/LDA+U approach is able to reproduce the experimental minimum band gaps of all four compounds to within 0.1 eV. These results, however, can only be achieved by applying extremely high cutoff parameters, which would be very difficult without using our recently developed accelerated GW approach. Our work demonstrates the applicability and accuracy of the G^0W^0/LDA+U method in predicting the quasiparticle band structure of these materials and other systems involving localized semicore states.

I. INTRODUCTION

The GW method[1–3] is one of the most successful and theoretically well-based methods for predicting the excited states properties of materials. Its predictive power is, however, sometimes obscured by several issues in practical calculations. For some materials (most simple *sp* materials including Si, Ge and GaAs), the calculated properties may appear to be fairly insensitive to various numerical cutoff parameters; for others (including, but not limited to, MgO, ZnO and the systems discussed in this work), under-converged results may lead to false predictions[4,5]. The convergence issue is further complicated by the fact that GW calculations are often computationally demanding, and imposing small cutoff parameters is sometimes not just a convenience but a requirement, especially for large and/or complex systems, and for materials containing localized semicore states. As we will show in this work, cuprous and silver halides are among the most challenging systems for GW quasiparticle calculations. In fact, these materials are sometimes (incorrectly) regarded as examples for which the widely used G^0W^0 (also known as one-shot GW)[2] approach fails to give accurate predictions.

The cuprous and silver halides are an interesting class of ionic semiconductors found in various applications. Cuprous halides (CuX: X = Cl, Br) form the end class of tetrahedrally coordinated binary semiconductors. These materials have attracted continuous research interest both for practical applications and understanding the fundamental semiconductor physics. CuCl is a wide gap semiconductor (quasipartcile gap E_g = 3.399 eV[6]) which has been actively studied for its unusual linear and nonlinear optical properties[6–10] including a large ex-

citon binding energy of over 190 meV[6,7] and an extremely sharp excitonic Z_3 peak[6]. AgCl and AgBr are the primary materials used in photographic and photochromatic applications.

Surprisingly, although the basic electronic structures of cuprous and silver halides have been studied by several groups[11–16] within density functional theory (DFT)[17,18], to the best of our knowledge, there have been no reports of systematic studies of the quasiparticle band structure of these materials using the GW method. It turns out that GW calculations for cuprous halides are significantly more challenging than the much discussed *extreme* case of ZnO[4,19,20]. In fact, a straightforward (but under-converged) G^0W^0 calculation starting from the Kohn-Sham local density approximation (LDA) solutions, which would normally give excellent results for simple *sp* materials such as Si or Ge, gives a quasiparticle band gap of about 1.6 eV for CuCl, to be compared with the experimental gap of 3.4 eV. Unfortunately, fully converged GW calculations for these materials using conventional methods are prohibitively expensive as we will show later.

We have recently implemented an efficient and accurate method[5] that can drastically speed up GW calculations, enabling fully converged GW calculations for complex systems at a fraction of computational cost compared with the conventional methods. In this work, we apply this new method to investigate the quasiparticle band structures of Cu and Ag halides, aiming at illustrating the difficulty of GW calculations for system involving localized d states and the importance of the convergence issue in GW calculations for these systems. We show that, once the calculations are fully converged, the LDA+U/G^0W^0 method is able to give very accurate results for systems with localized semicore states.

II.   COMPUTATIONAL DETAILS

TABLE I: Experimental lattice parameters used in this work. ZB stands for the zinc-blende structure, and RS for the rock-salt structure.

Property	AgCl	AgBr	CuCl	CuBr
Structure	RS	RS	ZB	ZB
Lattice const. (Å)	5.546[21]	5.772[21]	5.420[22]	5.696[22]

The pseudopotential plane wave based DFT calculations are carried out using the `PARATEC` package[23]. We use the Troullier-Martins norm-conserving pseudopotential[24]. Semicore electrons, namely, the $4s$, $4p$, and $4d$ electrons of silver and $3s$, $3p$, and $3d$ electrons of copper, are included in the calculations. In order to describe accurately the highly-localized semicore states, we used a 200 Ry plane wave cutoff for AgX and 250 Ry for CuX (X = Cl, Br). The experimental crystal structures used in this work are tabulated in Table I. The Brillouin zone integration is carried out using a 6×6×6 uniform k-grid.
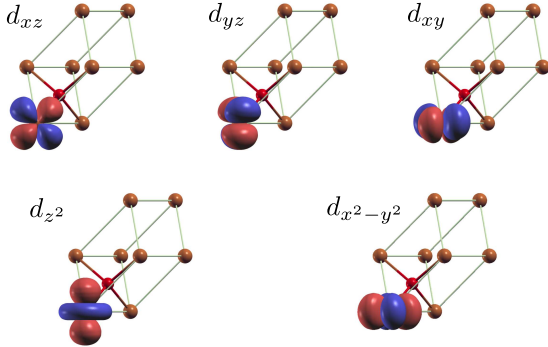

FIG. 1: Five maximally-localized Wannier functions optimized for copper d-states displaying the characters of spherical harmonics with $l = 2$. The top three Wannier functions have the t_2 symmetry, and the bottom two have the e symmetry.

The screened Coulomb U and exchange J used in the LDA+U[25,26] calculations are calculated using a recently developed method[27,28] that combines the constrained random phase approximation (cRPA)[29–32] and the maximally-localized Wannier functions (MLWF)[33] approaches. Briefly, we first calculate the dielectric function within the cRPA[27,28] and construct the MLWFs for the d states. The intrachannel polarizability is calculated using a wave-function projection technique[27,34]. The 5×5 U_{ij} and J_{ij} parameters are evaluated as

$$U_{ij} = \int d\mathbf{r}d\mathbf{r}' |\phi_i(\mathbf{r})|^2 W_c(\mathbf{r},\mathbf{r}') |\phi_j(\mathbf{r}')|^2, \qquad (1)$$

and

$$J_{ij} = \int d\mathbf{r}d\mathbf{r}' \phi_i^*(\mathbf{r})\phi_j^*(\mathbf{r}') W_c(\mathbf{r},\mathbf{r}') \phi_i(\mathbf{r}')\phi_j(\mathbf{r}), \qquad (2)$$

where i and j are the indices of the Wannier functions, and W_c is the screened Coulomb interaction calculated using the cRPA dielectric function[27]. The U and J parameters used in the LDA+U calculations are then given by: $U = \frac{1}{(2l+1)^2} \sum_{ij} U_{ij}$ and $J = \frac{1}{2l(2l+1)} \sum_{i \neq j} J_{ij}$, where $l = 2$ for d orbitals. These two parameters are then used to reconstruct the screened Coulomb and exchange matrix elements in the DFT+U[25,26,35] calculations as discussed in our previous work[36] and references therein. The calculated U and J parameters depend on the quality of the MLWFs ϕ_i, which should be optimized to closely resemble the features of subshell orbitals we are interested in. Figure 1 illustrates the constructed Wannier functions for copper $3d$ orbitals in CuBr, which clearly show the shapes and symmetry of the d orbitals.

TABLE II: Calculated screened Coulomb interaction parameter U and exchange interaction parameter J.

Parameter	AgCl	AgBr	CuCl	CuBr
U (eV)	5.2	5.0	6.1	6.1
J (eV)	0.6	0.6	0.9	0.8

Table II shows the calculated U and J parameters for the four compounds studied in this work. We mention that all U and J parameters are calculated self-consistently as discussed in our previous work[27]. Briefly, we first carry out DFT (i.e., by setting $U = J = 0$) calculations and evaluate the U and J parameters. These parameters are then used in subsequent DFT+U calculations and the U and J parameters are recalculated until the input and output parameters become the same. Simple linear extrapolations can greatly accelerate the convergence process. Overall, the Coulomb U for Cu $3d$ states is about 1 eV greater than that for Ag $4d$. Silver halides have almost the same U and J parameters, so do the cuprous halides.

The GW quasiparticle calculations are carried out using a local version of the `BerkeleyGW` package[37]. The recently developed acceleration technique[5] is employed to evaluate the summations over a large number of conduction bands. The Hybertsen-Louie generalized plasmon-pole model (HL-GPP)[2] is used to extend the static dielectric function to finite frequencies. The maximally localized Wannier functions (MLWF) are constructed using the `WANNIER90` package[38], and the quasiparticle band structures are calculated using the Wannier interpolation technique[33]. The spin-orbit coupling (SOC) effects are included as first-order perturbation[39–41] to the quasiparticle energies.
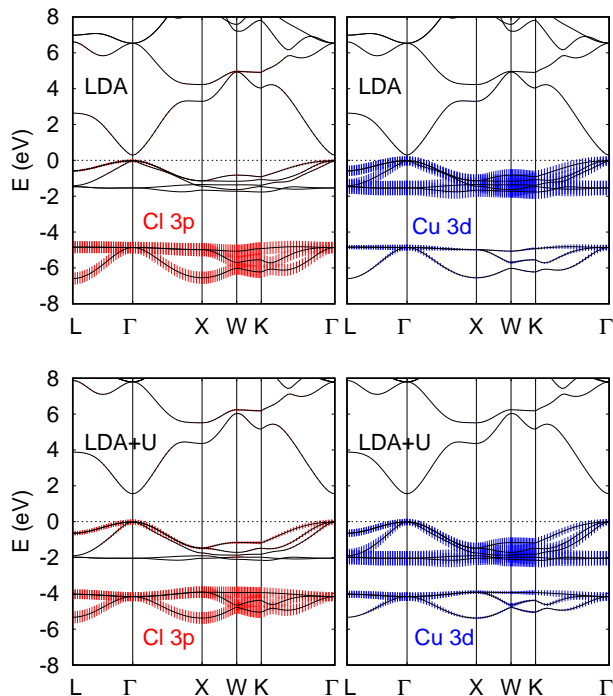
FIG. 2: Band structure of CuCl calculated within the LDA (top) and the LDA+U (bottom) methods. The projection of the Kohn-Sham wave functions onto the atomic Cl 3p (colored red) and Cu 3d (blue) states are shown as vertical bars superimposed on the band structures.

III.   RESULTS AND DISCUSSION

A.   The LDA and LDA+U band structures of CuCl and AgCl

Before we present the GW results, we would like to discuss some general features of the band structures of Cu and Ag halides calculated with the LDA and LDA+U functionals, using CuCl and AgCl as examples. It is well known that the LDA underestimates the binding energy of localized d states in semiconductors. In the case of ZnO, this under-binding of the Zn d states gives rise to strong pd hybridization which pushes the oxygen p states up, resulting in a very small LDA band gap of about 0.7 eV[4], to be compared with the experimental gap of about 3.6 eV[4,42,43] after correcting for the electron-phonon and excitonic effects. The LDA result for CuCl is even worse than that for ZnO.

The top panels of Fig.2 shows the projected band structure of CuCl calculated within the LDA. The top five valence bands are mainly of Cu 3d character and the bottom three valence bands are derived from the Cl 3p states. The under-binding of the Cu d bands is so severe that the LDA predicts a band gap of only 0.32 eV for CuCl, to be compared with the experimental gap of 3.40 eV. Not surprisingly, a straightforward (but under-converged) G^0W^0 calculation starting from the LDA Kohn-Sham solution

gives a GW band gap of about 1.6 eV for CuCl as we will discuss in detail later. For CuBr, the LDA band gap is 0.24 eV, to be compared with the experimental gap of 3.08 eV. The underestimation of the binding energy of the semicore d states also results in an inaccurate account of the pd hybridization effects in these materials, further complicating the reliability of the G^0W^0 approach.

In the bottom panels of Fig.2, we show the projected LDA+U band structure of CuCl. Compared with the LDA band structure, several important features are readily seen. First, the lowering of the d bands within the LDA+U method gives rise to a much larger DFT band gap of 1.48 eV for CuCl, which is more consistent with the typical accuracy of DFT results for semiconductors. In addition, the lowering of the d bands also results in an enhanced pd hybridization as can be seen from the figures. The top three valence bands now have appreciable Cl p components, and the bottom three valence bands have significant admixture of d components.
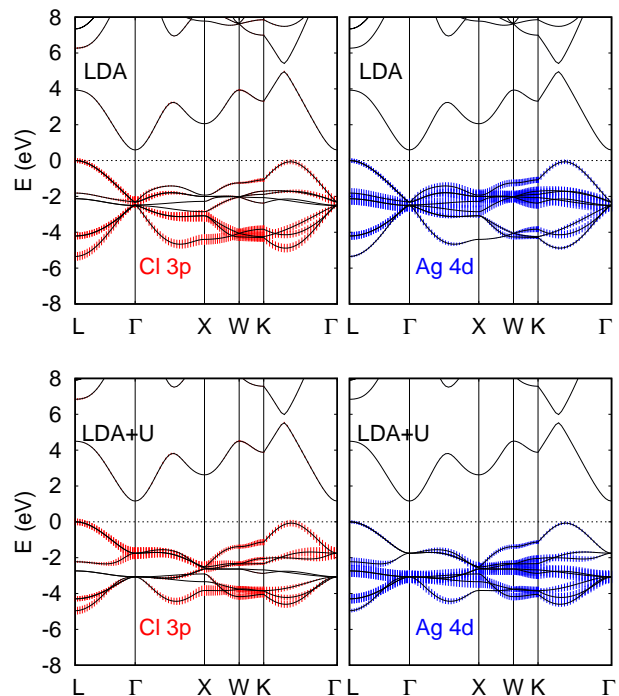

FIG. 3: Band structure of AgCl calculated within the LDA (top) and the LDA+U (bottom) methods. The projection of the Kohn-Sham wave functions onto the atomic Cl 3p and Ag 4d states are shown as vertical bars superimposed on the band structures.

Figure 3 compares the projected band structures of AgCl calculated using the LDA and the LDA+U functionals. AgCl assumes a rock-salt structure and has an L to Γ indirect band gap. The application of an on-site Coulomb U also results in a noticeable enhancement of the Cl p component in the top valence band and an increase (from 0.59 to 1.14 eV) in the calculated minimum indirect band gap. The eight hybridized pd valence states

are nearly degenerate at the Γ point within the LDA, which are separated into two groups, one with predominantly Cl p characters and the other Ag d within the LDA+U method. These changes, although significant, are not as dramatic as those observed for CuCl.

In our previous work[4], we showed that a combined LDA+U and G^0W^0 can accurately predict the quasiparticle band gap of ZnO as long as the calculations are adequately converged. In fact, this approach has been applied to several other systems[44–46] and showed very promising results. There are several motivations behind the use of the LDA+U solution as a starting point for subsequent GW calculations. The LDA+U approach describes better the localized d states and the pd hybridization, which significantly improve the quality of the quasiparticle wave functions. In addition, the LDA+U solution improves the calculated Kohn-Sham band gap, resulting in better dielectric screening properties. Table III compares the calculated macroscopic optical dielectric constants, $\epsilon_\infty = \lim_{\mathbf{q}\to 0} 1/\epsilon_{00}^{-1}(\mathbf{q})$, using the LDA and LDA+$U$ approaches with experiment. It is clear that the LDA+U approach gives results that better agree with experiment, particularly for CuCl and CuBr. Therefore, it is conceivable that GW calculations starting from the LDA+U solution be able to give better results compared with the G^0W^0/LDA approach for these systems.

TABLE III: Comparison between the calculated macroscopic dielectric constant with experiment.

ϵ_∞	AgCl	AgBr	CuCl	CuBr
LDA	5.4	6.6	18.5	54.6
LDA+U	5.3	6.2	4.4	5.2
Experiment	3.7[47], 3.97[48]	4.68[48]	3.61[49]	4.06[50]

B. Convergence behavior of the GW results for CuX and AgX

Conventional GW calculations involve two computationally expensive summations over conduction bands in calculating the dielectric function ϵ and the Coulomb-hole (COH) part of self-energy operator $\Sigma_{\mathrm{COH}}(E)$. For example, the COH matrix element[37] between states $|nk\rangle$ and $|n'k\rangle$ is

$$\langle n\mathbf{k}|\Sigma_{\mathrm{COH}}(E)|n'\mathbf{k}\rangle =$$

$$\frac{i}{2\pi}\sum_{n''}^{\substack{\text{all}\\\text{bands}}}\sum_{\mathbf{q}\mathbf{G}\mathbf{G}'} M_{n''n}^*(\mathbf{k},-\mathbf{q},-\mathbf{G})M_{n''n'}(\mathbf{k},-\mathbf{q},-\mathbf{G}')\times$$

$$\int_0^\infty dE' \frac{[\epsilon^r_{\mathbf{G},\mathbf{G}'}(\mathbf{q};E')]^{-1}-[\epsilon^a_{\mathbf{G},\mathbf{G}'}(\mathbf{q};E')]^{-1}}{E-E_{n''\mathbf{k}-\mathbf{q}}-E'+i\delta}V_c(\mathbf{q}+\mathbf{G}'),$$

where ϵ^r (ϵ^a) is the retarded (advanced) dielectric function, $M_{nn'}(\mathbf{k},\mathbf{q},\mathbf{G})=\langle n,\mathbf{k}+\mathbf{q}|e^{i(\mathbf{q}+\mathbf{G})}|n',\mathbf{k}\rangle$, and $V_c(\mathbf{q})$

is the Fourier transform of the bare Coulomb interaction. The above band summation should in principle include *all* conduction (empty) states in the Hilbert space of the Kohn-Sham Hamiltonian, and the dimension of the dielectric matrix should be the same as that of the Kohn-Sham Hamiltonian. In practice, however, truncations are almost always applied to both the band summation and the size (i.e., the kinetic energy cutoff) of the dielectric matrix.

The reason that GW calculations for systems involving localized d states are significantly more challenging than those for simple sp materials is two-fold. First, the convergence of GW results with respect to the number of conduction bands included in the calculations of both the dielectric function and the COH energy can be extremely slow for systems containing localized states, which means that one needs to include a very large number of bands in the summation to achieve reasonably converged results. Second, one also has to ensure that size of the dielectric matrix $\epsilon_{\mathbf{G},\mathbf{G}'}$ is large enough so that contributions to the correlation energy from high-G components are properly taken into account.

These convergence issues, if not properly addressed, can be a source of confusion since under-converged results reported by different groups may vary significantly. For large systems, it is extremely difficult (if possible at all) to perform fully converged GW calculations using the conventional band-by-band summation method. Our recently developed method[5] *effectively* allows including *all* conduction bands in GW calculations, enabling fully converged GW calculations at a fraction of the computational cost compared with the conventional method. We mention that for some systems, it is possible that the calculated quasiparticle band gap appears to converge well while the self-energy of neither the conduction band minimum (CBM) nor the valence band maximum (VBM) converges because of error cancellation. This can only happen when the CBM and VBM wave functions share similar characters. For systems such as ZnO, however, the wave function of the VBM states are derived from strongly localized atomic states (i.e., oxygen $2p$ states hybridized with Zn $3d$ states), whereas the CBM state (Zn $4s$) is highly delocalized. The convergence behavior of the calculated band gap is thus controlled by that of the localized VBM states. The situation here is actually more challenging than the much discussed *extreme* case of ZnO. For CuCl, the VBM states are mostly of Cu $3d$ character as we have discussed earlier (Fig.2), which are more localized than the oxygen $2p$ states.

Another issue is that, as a many-body perturbation method, the success of the G^0W^0 method relies on a faithful mean-field solution as a starting point. It is now well-established that the semilocal functionals within the local density approximation (LDA)[18] or generalized gradient approximation (GGA)[51–53] have difficulties in treating localized states, which may lead to an inaccurate description of the pd hybridization as we have discussed earlier.
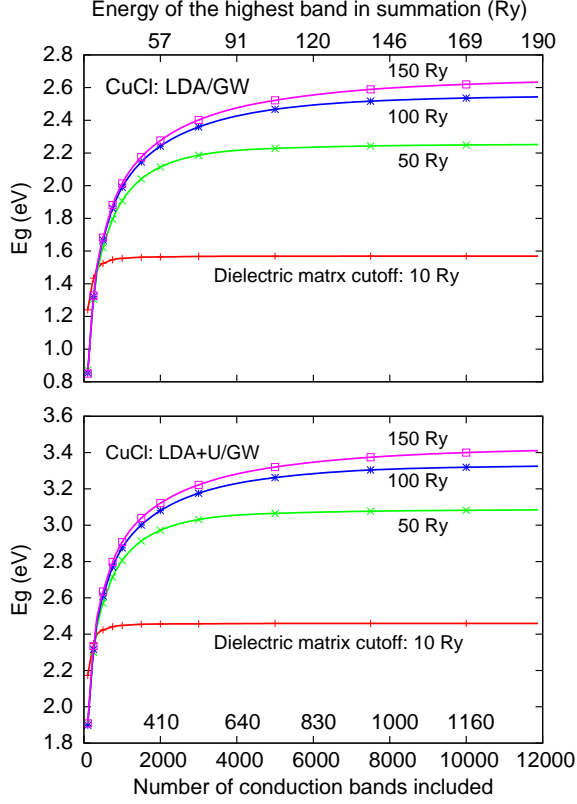
5

FIG. 4: Convergence behavior of the calculated GW band gap of CuCl: Comparison between the GW/LDA (upper panel) and the LDA+U (lower panel) approaches. See text for details about the horizontal labels.
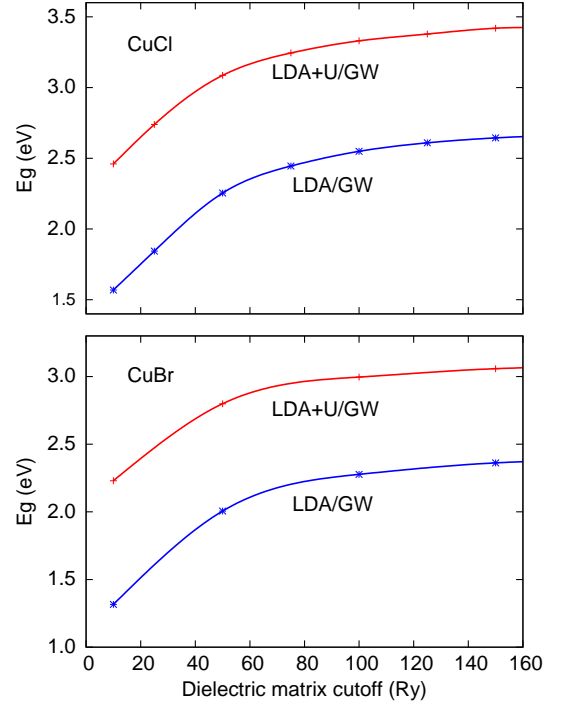

FIG. 5: Calculated band gaps of CuCl (upper panel) and CuBr (lower panel) using the GW/LDA (shown in blue) and LDA+U (red) approaches as a function of the kinetic energy cutoff of the dielectric matrix. The results in this figure are fully converged with respect to the number of bands included in the dielectric function and the COH energy calculations.

Figure 4 shows the convergence behavior of the calculated quasiparticle band gap of CuCl as a function of the number of empty states included in the GW calculations and the kinetic energy cutoff for the dielectric matrix. We have carried out GW calculation starting from both the LDA (upper panel) and LDA+U (lower panel) Kohn-Sham solutions. It is clear that an extremely high kinetic energy cutoff ($E_{\rm cut}^\epsilon = |G_{\rm cut}|^2/2$) for the dielectric matrix ($\epsilon_{\bf GG'}$) is needed to converge the calculated GW band gap. The calculated quasiparticle band gap converges to less than 1.6 eV if a small $E_{\rm cut}^\epsilon$ of 10 Ry is used and if the GW calculations are carried out on top of the LDA Kohn-Sham solution. A very large $E_{\rm cut}^\epsilon$ value of about 100 Ry is needed to converge the GW band gap to within 0.1 eV, or 150 Ry to within 0.02 eV.

Moreover, an enormous number of conduction bands has to be included in the band summation mentioned earlier to fully converge the band gap: About 8,000 bands are needed to converge the band gap of CuCl to within 0.05 eV, or 10,000 to within 0.02 eV. Carrying out the summation of $\sim 10,000$ bands in GW calculations is a formidable task even for these small systems. Our newly developed method[5] greatly alleviates such a burden by replacing the explicit band-by-band summation with an efficient energy integration for high energy con-

duction states. Using this method, we only need to carry out the summation/integration over about 1,000 bands to achieve the results that are equivalent to including 8,000 bands for GW calculations for CuCl. The number of bands included in our calculations are shown above the horizontal axis in Fig.4, whereas the number below the horizontal axis are the equivalent number of bands if the calculations were carried out using the conventional band-by-band summation method. We also show the kinetic energy of the highest conduction band included in the calculation in the figure (the horizontal scale at the top of the figure).

If the G^0W^0 calculations are carried out on top of the LDA mean-field solution, we obtain a fully converged band gap of about 2.66 eV (to be compared with the experimental gap of 3.4 eV) for CuCl as shown in Fig.4 and the upper panel of Fig.5, which is obviously far from satisfactory. On the hand other, if the GW calculations are performed on top of the LDA+U solutions, we obtain a fully converged gap of 3.42 eV (Fig.4 and the upper panel of Fig.5), which agrees perfectly with experiment. All results presented in Fig.5 are fully converged with respect to the number of bands included in the dielectric function and COH energy calculations

The results for CuBr are summarized in the lower panel of Fig.5. The general convergence behavior is similar to
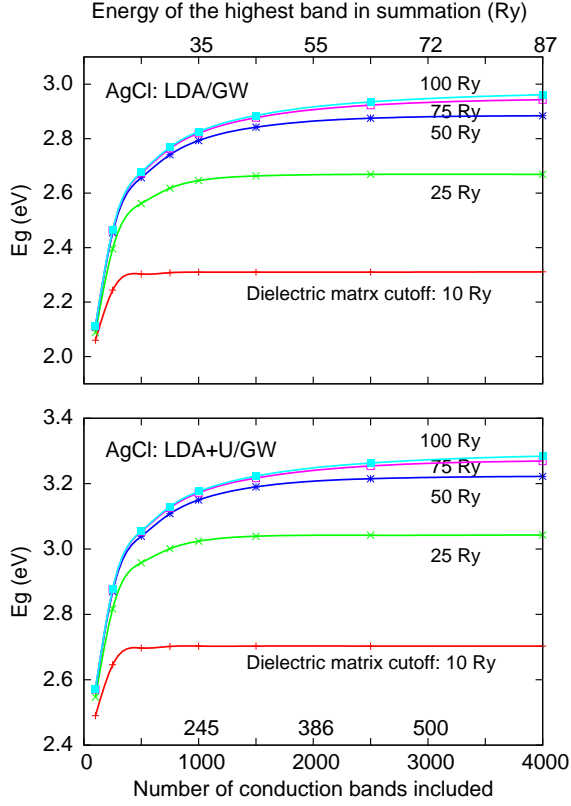
FIG. 6: Convergence behavior of the calculated GW band gap of AgCl: Comparison between the GW/LDA (upper panel) and the LDA+U (lower panel) approaches. The horizontal labels are the same as those shown in Fig.4 as discussed in the text.
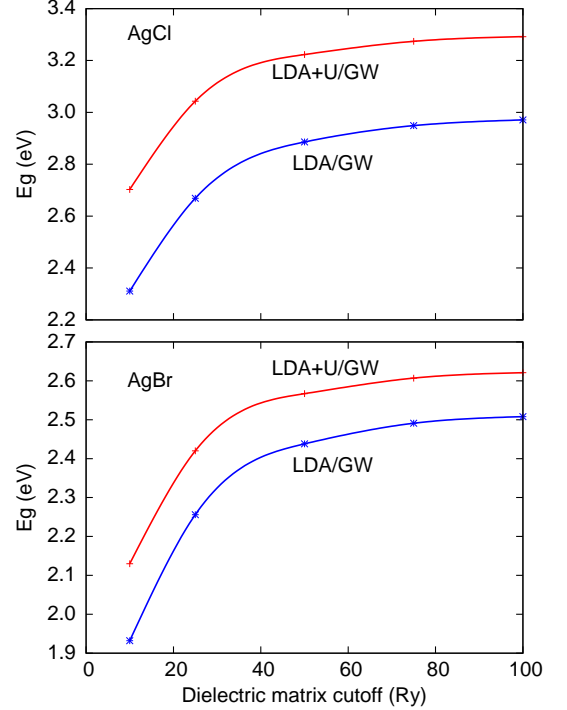

FIG. 7: Calculated band gaps of AgCl (upper panel) and AgBr (lower panel) using the GW/LDA (shown in blue) and LDA+U (red) approaches as a function of the kinetic energy cutoff of the dielectric matrix. The results in this figure are fully converged with respect to the number of bands included in the dielectric function and the COH energy calculations.

that for CuCl; therefore, we will not discuss the details here. Briefly, a small cutoff for the dielectric matrix and using the LDA solution as a starting point would give a GW gap of about 1.3 eV. Starting from the LDA+U solution, a fully converged G^0W^0 calculation gives a band gap of about 3.07 eV for CuBr, in excellent agreement with the experimental result of 3.08 eV[54]. Including the SOC effects reduces the minimum gap slightly. We will come back to this point later.

We would like to mention that the convergence issue discussed here is not just limited to plane-wave based GW methods. In fact, atomic orbital based methods should suffer from the same problem. However, since the dimension of the Hilbert space is severely limited and far from complete in atomic orbital based methods, one would not be able to carry out similar convergence tests as we show here. In other words, if the GW calculations are carried out within a restricted basis set, one may observe a false convergence behavior.

We now discuss the convergence behavior of the GW results for silver halides. AgCl and AgBr both have an indirect band gap with the VBM located at the L point and the CBM at the Γ point as shown in Fig.3. The VBM states are mainly of Cl $3p$ character with some

hybridization with silver $4d$ states. Both the Cl $3p$ and silver $4d$ states are considerably more extended compared with the Cu $3d$ states. Therefore, we expect that the convergence issues discussed above for CuX remain valid but to a much lesser extent for AgX.

Figure 6 shows the convergence behavior of the calculated minimum (L to Γ) indirect band gap of AgCl without including the SOC effects. Results including the SOC splitting will be discussed later. We find that an kinetic energy cutoff of 70 Ry for the dielectric matrix is sufficient to converge the calculated band gap to within 0.02 eV, compared with about 150 Ry for CuCl to achieve the same level of convergence. The band-convergence issue is also significantly less severe than that observed for CuCl; one only needs to include about 2,500 empty states in the GW calculations for AgCl. Using our new method[5], this number is effectively reduced to about 440. Whether the GW calculations are carried out starting from the LDA or LDA+U solution also has noticeable effects: The GW/LDA approach gives a band gap of 2.97 eV, whereas the GW/LDA+U approach gives a band gap of 3.29 eV. Figure 7 summarizes the convergence behavior of the calculated indirect minimum gap of AgCl and AgBr as a function of the kinetic energy cutoff of the dielectric matrix using the GW/LDA and GW/LDA+U approaches. The results are fully converged with respect

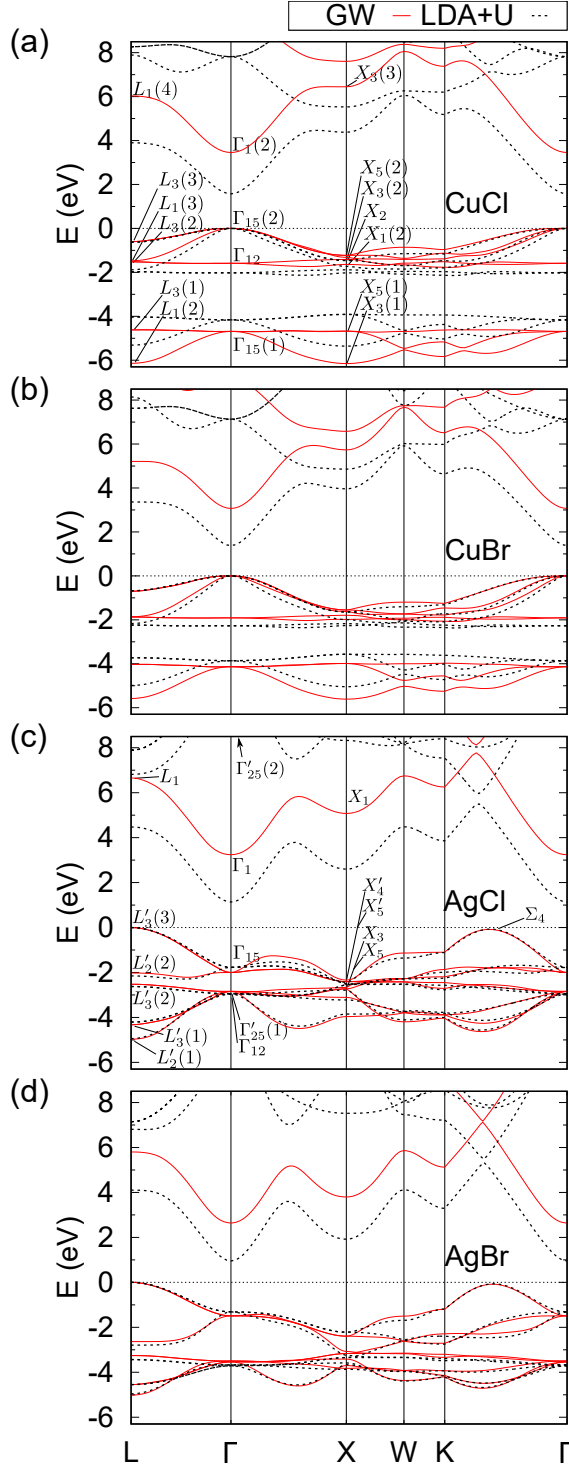to the number of bands included in the dielectric function and the COH energy calculations.

FIG. 8: Fully converged quasiparticle band structures of Cu and Ag halides calculated using the GW/LDA+U approach. The LDA+U band structures are also shown with dashed line for comparison. Spin-orbit coupling effects are not included in the figures for clarity.

C. Quasiparticle band structures of CuX and AgX: Comparison between theory and experiment

Figure 8 shows the fully converged quasiparticle band structures of all four systems. The labeling of the states at the high-symmetry points follows the convention of Ref.[11] and Ref.[61]. The GW band structures are calculated using the Wannier interpolation method[33] with the results calculated on a $6 \times 6 \times 6$ k-grid. The band structures for CuCl and CuBr share interesting similarities, so do those of AgCl and AgBr. The upper five valence bands are separated from the lower three with a sizable gap for cuprous halides, whereas for silver halides, the eight valence bands are strongly entangled. It is interesting to note that the Σ hole-valley, which locates along the $K \to \Gamma$ direction, is nearly degenerate with the VBM ($L_3(3)'$) for both AgCl and AgBr. Figure 9 compares the GW band structures of AgCl and AgBr, with and without including the SOC effects. The SOC effects in Cu halides are not as significant as those in Ag halides.
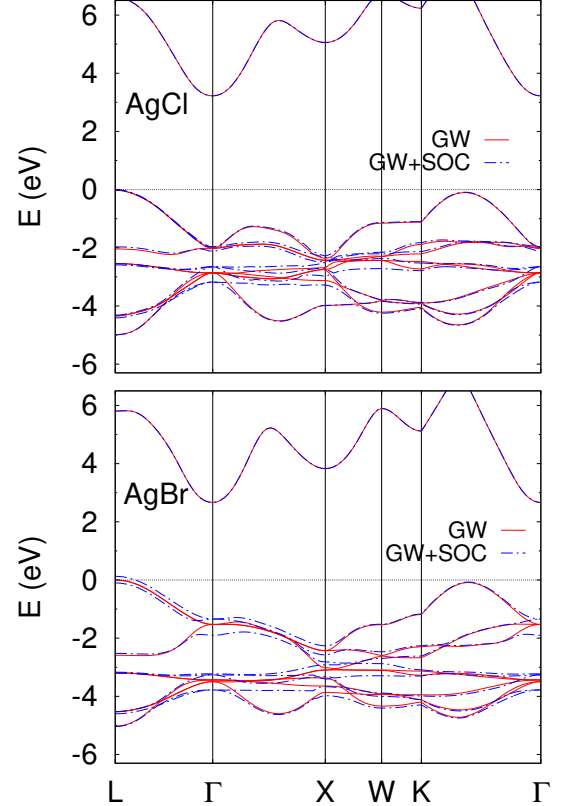

FIG. 9: Quasiparticle band structures of AgCl and AgBr with and without including the SOC effects.

Table IV summarizes the calculated GW band gaps and comparison with available experiments and previous theoretical results. For CuCl and CuBr, the experimental values quoted in the table are the quasiparticle gaps, whereas for AgCl and AgBr, we compare with op-

TABLE IV: Comparison between the calculated quasiparticle band gap (in eV) with previous theory and available experiments. For silver halides, we present the direct band gap E_g^{dir} at the Γ point and the indirect band gap E_g^{ind} from L to Γ. Results including the SOC splitting are shown with curly brackets. We also include some experimental results which do not resolve the SOC splitting. The experimental results for copper halides are the quasiparticle excitation results, whereas the experimental data for silver halides are taken from optical measurements which include excitonic effects.

Material		Previous Theory			This Work					Experiment
		LDA	GGA	HSE	LDA	LDA+U	GW (LDA)	GW (LDA+U)	GW+SOC (LDA+U)	
CuCl	E_g^{dir}	—	0.51[a]	2.76[e]	0.32	1.48	2.66	3.42	3.39 } 3.42	3.40 } 3.46 ∼ 3.47 [b]
CuBr	E_g^{dir}	—	0.42[a]	2.76[e]	0.24	1.38	2.38	3.07	2.98 } 3.22	3.08 } 3.23 [c]
AgCl	E_g^{dir}	3.35[d]	3.09[d]	4.49[e]	2.91	2.91	5.05	5.30	5.25 } 5.40	5.10 ∼ 5.15 [fg]
	E_g^{ind}	0.64[d]	0.94[d]	2.60[e]	0.59	1.13	2.97	3.29	3.27 } 3.38	3.25[f] 3.26 } 3.31 [h]
AgBr	E_g^{dir}	2.60[d]	2.43[d]	3.78[e]	2.27	2.27	4.07	4.17	3.99 } 4.55	4.29[f] 3.9 ∼ 4.25 } 4.3 ∼ 4.85 [ih]
	E_g^{ind}	0.39[d]	0.68[d]	2.24[e]	0.38	0.81	2.51	2.64	2.52 } 2.75	2.69[f] 2.70 } 2.85 [h]

[a]Ref.[14]
[b]Ref.[6] and Ref.[54] and Ref.[55]
[c]Ref.[54] and Ref.[56]
[d]Ref.[16]
[e]Ref.[15]
[f]Ref.[57]
[g]Ref.[58]
[h]Ref.[59]
[i]Ref.[60]

tical measurement. Some of the results have been discussed earlier, so we will not repeat here. Results including the SOC splitting are shown with curly brackets. We also include experimental results that do not resolve the SOC splitting. For CuCl and CuBr, the converged GW results calculated starting from the LDA+U solution agree extremely well with experiments, whereas the results obtained from the GW/LDA approach (even fully converged) significantly underestimate the band gap (by about 0.7 eV). For AgCl and AgBr, the GW/LDA+U approach also gives considerably improved minimum indirect gap (E_g^{ind}) compared with experiments. The GW/LDA approach predicts the E_g^{ind} of AgCl to be 2.97 eV, which is about 0.3 eV smaller than the experimental value. For the direct gap at Γ (E_g^{dir}), however, such an improvement is not clear due to large uncertainties of the experimental results. For example, the measured direct gap at Γ (E_g^{dir}) of AgBr has a very large variation of 0.6 eV. Thus our results call for further experimental verifications.

In addition to the band gaps, we also compare the calculated quasiparticle energies at high symmetry points with experimental values. Table V compares the calculated quasiparticle energies (measured from the VBM) of CuCl at the Γ, X, and L points with experiments.

The labeling of the electronic states are shown in Fig.8. Overall, the GW/LDA+U approach gives significantly improved results compared with the LDA+U approach. There are a few exceptions, however. For example, for the Γ_{12} state, the LDA+U method predicts an energy of -2.0 eV, which is surprisingly close to the experimental value of -1.9 eV. The GW/LDA+U approach, however, predicts an energy of -1.66 eV.

Table VI compares the calculated quasiparticle energies (measured from the VBM) for CuBr at the Γ and L points with angle-resolved photoemission experiments. The SOC effects are included using a perturbation approach[39–41]. For most states, it is clear that the results calculated with the GW/LDA+U method agree better with experiments compared with those calculated with the LDA+U method. One exception is the energy of the $L_1(3)$ state. The GW/LDA+U predicts an energy of -1.98 eV whereas the measured value is -1.4 ± 0.3 eV. Since these are the first systematic quasiparticle band structure calculations for these materials and there seem to be large uncertainties in the experimental measurements and assignments, we call for more future experiments to compare with our theory. For AgCl and AgBr, we compare the state-to-state transition energy (i.e., the energy difference between two states involved) with optical measurements as shown in Table VII. Results includ-

TABLE V: Comparison between the experimental values and the calculated quasiparticle energies (in eV) of CuCl. All the energies are referenced from the VBM. The labeling of states follow the convention of Ref.[11] and Ref.[61].

States	LDA+U	GW (LDA+U)	Expt.
$\Gamma_1(2)$	1.48	3.42	3.40^a
$\Gamma_{15}(2)$	0.00	0.00	0.00
Γ_{12}	−2.00	−1.66	-1.9^{bc}
$\Gamma_{15}(1)$	−4.23	−4.73	-4.9^b
$X_1(3)$	5.43	7.57	7.8^d
$X_5(2)$	−1.44	−1.25	$-1.0^b, -1.3^c$
$X_3(2)$	−1.71	−1.38	-1.5^{bc}
X_2	−1.85	−1.50	-1.5^b
$X_1(2)$	−1.99	−1.68	-1.9^b
$X_5(1)$	−4.00	−4.69	$-4.9^b, -5.1^c$
$X_3(1)$	−5.45	−6.16	$-6.1^b, -6.9^c$
$L_3(3)$	−0.63	−0.61	$-0.6^b, -1.0^c$
$L_1(3)$	−1.85	−1.51	$-1.9^b, -1.5^c$
$L_3(2)$	−1.93	−1.58	-1.9^b
$L_3(1)$	−4.10	−4.65	$-4.9^b, -4.6^c$
$L_1(2)$	−5.43	−6.15	$-6.1^b, -6.8^c$

^{a}Ref.[6]
^{b}Ref.[62]
^{c}Ref.[54]
^{d}Ref.[61]

ing the SOC effects are presented in curly brackets. Experimentally, the assignments of some optical transitions are still not settled. In addition, there are significant uncertainties in the experimental values. These experimental issues, coupled with the excitonic effects, make it difficult to compare directly our theoretical results and experiment. We hope future theoretical calculations including excitonic effects and high resolution experiments can help to resolve these issues.

D. Some remarks

Quasiparticle GW calculations carried out by different groups can sometimes give significantly different results depending on the specific implementation and various convergence (truncation) parameters used in the calculations. The fact that the G^0W^0/LDA+U approach, in particular, with the use of the HL-GPP model, seems to consistently produce reasonable results for these and many other systems does not necessarily imply that this approach captures all physics the best way possible. In fact, G^0W^0 methods that do not use the plasmon-pole approximation (e.g., the contour deformation method[20]) cannot reproduce the experimental gap of ZnO. Therefore, some fortuitous error cancellation must be in play here. It appears that the LDA/GGA Kohn-Sham mean-field solution overestimates the screening effect; the error

arised from this factor seems to be rather well compensated by the HL-GPP model for various semiconductors.

There are several other issues that deserve some discussion. First, it is our understanding that self-consistent GW methods[66,67] often overestimate[68,69] the quasiparticle band gap of semiconductors. This overestimation will likely be greater than those reported if the results are fully converged with respect to the truncation parameters discuss in this work. Same can be said for GW calculations starting from the Kohn-Sham solution calculated using hybrid functionals. For example, it is shown[70] that the band gap of α-Fe_2O_3 is significantly overestimated with the use of hybrid functionals. These approaches suffer the same convergence issues we discuss here and should be carefully examined as well. Second, even within the G^0W^0/DFT approach, the effects of off-diagonal self-energy matrix elements deserve further investigation. Third, the use of pseudopotential may introduce fictitious exchange-correlation effects due to the very nature of the pseudo wavefunctions. We would like to caution, however, that doing fully converged all-electron GW calculations may be prohibitively expensive and difficult. Finally, there are electron-phonon self-energy effects[71,72] and polaronic polarization effects[73–76] which we do not consider in this work.

A full investigation of all of the above mentioned issues is clearly beyond the scope of this work. However, regardless of the specific GW implementation and the level of approximations used by different groups, the convergence issues we discuss here are always relevant. The fact that the pseudopotential G^0W^0 approach, in particular, when the HL-GPP model is used, gives results that agree with experiment maybe a result of a fortuitous combination of several factors. This issue certainly deserves future studies.

IV. SUMMARY

In summary, we have carried out GW calculations for CuCl, CuBr, AgCl, and AgBr and carefully analyzed the convergence of the GW results with respect to various parameters, especially the number of conduction bands included in the calculations and the kinetic energy cutoff for the dielectric matrices. Our results reveal the extreme difficulty for converging the calculated GW quasiparticle energies for cuprous halides. Our recent development in speeding up GW calculations has greatly alleviated the computational requirements for these materials. We also compare GW calculations carried out using the LDA and LDA+U mean-field solutions as starting points. We find that, once fully converged, the GW/LDA+U approach gives accurate predictions of the quasiparticle band gaps for these materials to within 0.1 eV compared with experiments, while the GW/LDA approach significantly underestimates the band gaps of cuprous halides due to the inaccurate account for the Coulomb correlation of d electrons, which in turn

TABLE VI: Quasiparticle enegies (in eV) of CuBr at the high-symmetry k points. All energies are referenced from the VBM. The double-group labeling of the states are also presented.

State		LDA+U	GW+SOC (LDA+U)	Expt.[a]
Γ_{12}	Γ_8	-2.27	-2.00	-2.05 ± 0.1
$\Gamma_{15}(1)$	$\begin{cases} \Gamma_8 \\ \Gamma_7 \end{cases}$	-3.86	$\begin{cases} -4.18 \\ -4.34 \end{cases}$	$\begin{cases} -4.2 \pm 0.2 \\ -4.8 \pm 0.3 \end{cases}$
$L_3(3)$	$\begin{cases} L_{4,5} \\ L_6 \end{cases}$	-0.68	$\begin{cases} -0.74 \\ -0.82 \end{cases}$	-0.8 ± 0.3
$L_1(3)$	L_6	-2.17	-1.98	-1.4 ± 0.3
$L_3(2)$	$\begin{cases} L_{4,5} \\ L_6 \end{cases}$	-2.24	$\begin{cases} -1.92 \\ -2.11 \end{cases}$	-2.05 ± 0.1
$L_3(1)$	$\begin{cases} L_{4,5} \\ L_6 \end{cases}$	-3.73	$\begin{cases} -4.09 \\ -4.16 \end{cases}$	$\begin{cases} -4.2 \pm 0.2 \\ -4.7 \pm 0.3 \end{cases}$
$L_1(2)$	L_6	-4.99	-5.69	-5.6 ± 0.3

[a]Ref.[63]

TABLE VII: Comparison between theory and experiment the transition energies (in eV) for AgBr and AgCl. The notations for the states are shown in Fig. 8 (c).

Transition	LDA+U	GW+SOC (LDA+U)	Expt.
AgCl			
$X_5' \rightarrow X_1$	5.1	$\begin{cases} 7.39 \\ 7.51 \end{cases}$	7.15^a
$L_3'(3) \rightarrow L_1$	4.5	$\begin{cases} 6.63 \\ 6.65 \end{cases}$	6.25^b, 7.05^c
AgBr			
$X_4' \rightarrow X_1$	5.1	6.7	$5.8 \sim 7.3^c$
$X_5' \rightarrow X_1$	4.1	$\begin{cases} 6.03 \\ 6.34 \end{cases}$	
$L_3'(3) \rightarrow L_1$	4.1	$\begin{cases} 5.67 \\ 5.90 \end{cases}$	$5.1 \sim 5.7^c$

[a]Ref.[60]
[b]Ref.[59]
[c]Ref.[60,64,65]

results in a wrong description of the energy of d states and pd hybridization. Our results demonstrate the applicability and affordability of the GW/LDA+U approach for predicting the quasiparticle properties of these *hard-to-calculate* systems, in particular when this approach is combined with our recently developed accelerated GW method.

* Electronic address: pzhang3@buffalo.edu
[1] L. Hedin, Phys. Rev. **139**, A796 (1965), URL https://link.aps.org/doi/10.1103/PhysRev.139.A796.
[2] M. S. Hybertsen and S. G. Louie, Phys. Rev. B **34**, 5390 (1986), URL http://link.aps.org/doi/10.1103/PhysRevB.34.5390.
[3] R. W. Godby, M. Schlüter, and L. J. Sham, Phys. Rev. B **37**, 10159 (1988), URL https://link.aps.org/doi/10.1103/PhysRevB.37.10159.

[4] B.-C. Shih, Y. Xue, P. Zhang, M. L. Cohen, and S. G. Louie, Phys. Rev. Lett. **105**, 146401 (2010), URL http://link.aps.org/doi/10.1103/PhysRevLett.105.146401.

[5] W. Gao, W. Xia, X. Gao, and P. Zhang, Scientific Reports **6**, 36849 (2016), article, URL http://dx.doi.org/10.1038/srep36849.

[6] K. Saito, M. Hasuo, T. Hatano, and N. Nagasawa, Solid State Communications **94**, 33 (1995), URL http://www.sciencedirect.com/science/article/pii/0038109895000070.

[7] E. Hanamura, Phys. Rev. B **37**, 1273 (1988), URL https://link.aps.org/doi/10.1103/PhysRevB.37.1273.

[8] Z. K. Tang, A. Yanase, T. Yasui, Y. Segawa, and K. Cho, Phys. Rev. Lett. **71**, 1431 (1993), URL https://link.aps.org/doi/10.1103/PhysRevLett.71.1431.

[9] Y. Masumoto, T. Wamura, and A. Iwaki, Applied Physics Letters **55**, 2535 (1989), URL http://dx.doi.org/10.1063/1.102271.

[10] D. C. Haueisen and H. Mahr, Phys. Rev. B **8**, 734 (1973), URL https://link.aps.org/doi/10.1103/PhysRevB.8.734.

[11] A. Zunger and M. L. Cohen, Phys. Rev. B **20**, 1189 (1979), URL http://link.aps.org/doi/10.1103/PhysRevB.20.1189.

[12] R. H. Victora, Phys. Rev. B **56**, 4417 (1997), URL http://link.aps.org/doi/10.1103/PhysRevB.56.4417.

[13] G. Nunes, P. Allen, and J. Martins, Solid State Communications **105**, 377 (1998), URL http://www.sciencedirect.com/science/article/pii/S0038109897101477.

[14] B. Amrani, T. Benmessabih, M. Tahiri, I. Chiboub, S. Hiadsi, and F. Hamdache, Physica B: Condensed Matter **381**, 179 (2006), URL http://www.sciencedirect.com/science/article/pii/S092145260600189X.

[15] J. E. Peralta, J. Heyd, G. E. Scuseria, and R. L. Martin, Phys. Rev. B **74**, 073101 (2006), URL http://link.aps.org/doi/10.1103/PhysRevB.74.073101.

[16] T. Benmessabih, B. Amrani, F. E. H. Hassan, F. Hamdache, and M. Zoaeter, Physica B: Condensed Matter **392**, 309 (2007), URL http://www.sciencedirect.com/science/article/pii/S0921452606018564.

[17] P. Hohenberg and W. Kohn, Phys. Rev. **136**, B864 (1964), URL https://link.aps.org/doi/10.1103/PhysRev.136.B864.

[18] W. Kohn and L. J. Sham, Phys. Rev. **140**, A1133 (1965), URL https://link.aps.org/doi/10.1103/PhysRev.140.A1133.

[19] C. Friedrich, M. C. Müller, and S. Blügel, Phys. Rev. B **83**, 081101 (2011), URL http://link.aps.org/doi/10.1103/PhysRevB.83.081101.

[20] M. Stankovski, G. Antonius, D. Waroquiers, A. Miglio, H. Dixit, K. Sankaran, M. Giantomassi, X. Gonze, M. Côté, and G.-M. Rignanese, Phys. Rev. B **84**, 241201 (2011), URL http://link.aps.org/doi/10.1103/PhysRevB.84.241201.

[21] S. Hull and D. A. Keen, Phys. Rev. B **59**, 750 (1999), URL http://link.aps.org/doi/10.1103/PhysRevB.59.750.

[22] S. Hull and D. A. Keen, Phys. Rev. B **50**, 5868 (1994), URL http://link.aps.org/doi/10.1103/PhysRevB.50.5868.

[23] Accessed: 2015-07-28, URL http://www.nersc.gov/users/software/applications/materials-science/paratec/.

[24] N. Troullier and J. L. Martins, Phys. Rev. B **43**, 1993 (1991), URL http://link.aps.org/doi/10.1103/PhysRevB.43.1993.

[25] V. I. Anisimov, J. Zaanen, and O. K. Andersen, Phys. Rev. B **44**, 943 (1991), URL https://link.aps.org/doi/10.1103/PhysRevB.44.943.

[26] V. I. Anisimov, F. Aryasetiawan, and A. I. Lichtenstein, Journal of Physics: Condensed Matter **9**, 767 (1997), URL http://stacks.iop.org/0953-8984/9/i=4/a=002.

[27] B.-C. Shih, Y. Zhang, W. Zhang, and P. Zhang, Phys. Rev. B **85**, 045132 (2012), URL http://link.aps.org/doi/10.1103/PhysRevB.85.045132.

[28] B.-C. Shih, T. A. Abtew, X. Yuan, W. Zhang, and P. Zhang, Phys. Rev. B **86**, 165124 (2012), URL http://link.aps.org/doi/10.1103/PhysRevB.86.165124.

[29] M. Springer and F. Aryasetiawan, Phys. Rev. B **57**, 4364 (1998), URL https://link.aps.org/doi/10.1103/PhysRevB.57.4364.

[30] F. Aryasetiawan, M. Imada, A. Georges, G. Kotliar, S. Biermann, and A. I. Lichtenstein, Phys. Rev. B **70**, 195104 (2004), URL https://link.aps.org/doi/10.1103/PhysRevB.70.195104.

[31] F. Aryasetiawan, K. Karlsson, O. Jepsen, and U. Schönberger, Phys. Rev. B **74**, 125106 (2006), URL https://link.aps.org/doi/10.1103/PhysRevB.74.125106.

[32] T. Miyake, F. Aryasetiawan, and M. Imada, Phys. Rev. B **80**, 155134 (2009), URL http://link.aps.org/doi/10.1103/PhysRevB.80.155134.

[33] I. Souza, N. Marzari, and D. Vanderbilt, Phys. Rev. B **65**, 035109 (2001), URL https://link.aps.org/doi/10.1103/PhysRevB.65.035109.

[34] E. Şaşıoğlu, C. Friedrich, and S. Blügel, Phys. Rev. B **83**, 121101 (2011), URL https://link.aps.org/doi/10.1103/PhysRevB.83.121101.

[35] V. I. Anisimov, I. V. Solovyev, M. A. Korotin, M. T. Czyżyk, and G. A. Sawatzky, Phys. Rev. B **48**, 16929 (1993), URL https://link.aps.org/doi/10.1103/PhysRevB.48.16929.

[36] P. Zhang, W. Luo, V. H. Crespi, M. L. Cohen, and S. G. Louie, Phys. Rev. B **70**, 085108 (2004), URL https://link.aps.org/doi/10.1103/PhysRevB.70.085108.

[37] J. Deslippe, G. Samsonidze, D. A. Strubbe, M. Jain, M. L. Cohen, and S. G. Louie, Computer Physics Communications **183**, 1269 (2012), URL http://www.sciencedirect.com/science/article/pii/S0010465511003912.

[38] A. A. Mostofi, J. R. Yates, G. Pizzi, Y.-S. Lee, I. Souza, D. Vanderbilt, and N. Marzari, Computer Physics Communications **185**, 2309 (2014), URL http://www.sciencedirect.com/science/article/pii/S001046551400157X.

[39] M. Hybertsen and S. Louie, Phys. Rev. B **34**, 2920 (1986).

[40] B. D. Malone and M. L. Cohen, Journal of Physics: Condensed Matter **25**, 105503 (2013), URL http://stacks.iop.org/0953-8984/25/i=10/a=105503.

[41] W. Gao, X. Gao, T. A. Abtew, Y.-Y. Sun, S. Zhang, and P. Zhang, Phys. Rev. B **93**, 085202 (2016), URL http://link.aps.org/doi/10.1103/PhysRevB.93.085202.

[42] S. Tsoi, X. Lu, A. K. Ramdas, H. Alawadhi, M. Grimsditch, M. Cardona, and R. Lauck, Phys. Rev. B **74**, 165203 (2006), URL https://link.aps.org/doi/10.1103/PhysRevB.74.165203.

[43] H. Alawadhi, S. Tsoi, X. Lu, A. K. Ramdas, M. Grimsditch, M. Cardona, and R. Lauck, Phys. Rev. B **75**, 205207 (2007), URL https://link.aps.org/doi/10.1103/PhysRevB.75.205207.

[44] T. Miyake, P. Zhang, M. L. Cohen, and S. G. Louie, Phys. Rev. B **74**, 245213 (2006), URL http://link.aps.org/doi/10.1103/PhysRevB.74.245213.

[45] E. Kioupakis, P. Zhang, M. L. Cohen, and S. G. Louie, Phys. Rev. B **77**, 155114 (2008), URL https://link.aps.org/doi/10.1103/PhysRevB.77.155114.

[46] Y. Zhang, X. Yuan, X. Sun, B.-C. Shih, P. Zhang, and W. Zhang, Phys. Rev. B **84**, 075127 (2011), URL https://link.aps.org/doi/10.1103/PhysRevB.84.075127.

[47] T. Nakayama, S. Tamura, T. Yagi, K. Wakamura, M. Sugioka, K. Kawakami, and M. Kurita, Physica B: Condensed Matter **219**, 457 (1996), ISSN 0921-4526, URL http://www.sciencedirect.com/science/article/pii/0921452695007776.

[48] R. P. Lowndes, Phys. Rev. B **6**, 4667 (1972), URL http://link.aps.org/doi/10.1103/PhysRevB.6.4667.

[49] A. Feldman and D. Horowitz, J. Opt. Soc. Am. **59**, 1406 (1969), URL http://www.osapublishing.org/abstract.cfm?URI=josa-59-11-1

[50] E. H. Turner, I. P. Kaminow, and C. Schwab, Phys. Rev. B **9**, 2524 (1974), URL http://link.aps.org/doi/10.1103/PhysRevB.9.2524.

[51] D. C. Langreth and M. J. Mehl, Phys. Rev. B **28**, 1809 (1983), URL https://link.aps.org/doi/10.1103/PhysRevB.28.1809.

[52] J. P. Perdew, J. A. Chevary, S. H. Vosko, K. A. Jackson, M. R. Pederson, D. J. Singh, and C. Fiolhais, Phys. Rev. B **46**, 6671 (1992), URL https://link.aps.org/doi/10.1103/PhysRevB.46.6671.

[53] J. P. Perdew, K. Burke, and M. Ernzerhof, Phys. Rev. Lett. **77**, 3865 (1996), URL https://link.aps.org/doi/10.1103/PhysRevLett.77.3865.

[54] A. Goldmann, physica status solidi (b) **81**, 9 (1977), URL http://dx.doi.org/10.1002/pssb.2220810102.

[55] A. Göbel, T. Ruf, M. Cardona, C. T. Lin, J. Wrzesinski, M. Steube, K. Reimann, J.-C. Merle, and M. Joucla, Phys. Rev. B **57**, 15183 (1998), URL https://link.aps.org/doi/10.1103/PhysRevB.57.15183.

[56] M. Cardona, Phys. Rev. **129**, 69 (1963), URL http://link.aps.org/doi/10.1103/PhysRev.129.69.

[57] M. G. Mason, Phys. Rev. B **11**, 5094 (1975), URL http://link.aps.org/doi/10.1103/PhysRevB.11.5094.

[58] N. J. Carrera and F. C. Brown, Phys. Rev. B **4**, 3651 (1971), URL https://link.aps.org/doi/10.1103/PhysRevB.4.3651.

[59] F. Bassani, R. S. Knox, and W. B. Fowler, Phys. Rev. **137**, A1217 (1965), URL http://link.aps.org/doi/10.1103/PhysRev.137.A1217.

[60] J. J. White, J. Opt. Soc. Am. **62**, 212 (1972), URL http://www.osapublishing.org/abstract.cfm?URI=josa-62-2-212.

[61] A. Goldmann and D. Westphal, Journal of Physics C: Solid State Physics **16**, 1335 (1983), URL http://stacks.iop.org/0022-3719/16/i=7/a=019.

[62] D. Westphal and A. Goldmann, Journal of Physics C: Solid State Physics **15**, 6661 (1982), URL http://stacks.iop.org/0022-3719/15/i=32/a=026.

[63] R. Matzdorf, J. Skonieczny, J. Westhof, H. Engelhard, and A. Goldmann, Journal of Physics: Condensed Matter **5**, 3827 (1993), URL http://stacks.iop.org/0953-8984/5/i=23/a=009.

[64] J. J. White and J. W. Straley, J. Opt. Soc. Am. **58**, 759 (1968), URL http://www.osapublishing.org/abstract.cfm?URI=josa-58-6-759.

[65] R. S. Bauer, W. E. Spicer, and J. J. White, J. Opt. Soc. Am. **64**, 830 (1974), URL http://www.osapublishing.org/abstract.cfm?URI=josa-64-6-830.

[66] M. van Schilfgaarde, T. Kotani, and S. Faleev, Phys. Rev. Lett. **96**, 226402 (2006), URL https://link.aps.org/doi/10.1103/PhysRevLett.96.226402.

[67] M. Shishkin and G. Kresse, Phys. Rev. B **75**, 235102 (2007), URL http://link.aps.org/doi/10.1103/PhysRevB.75.235102.

[68] H. Cao, Z. Yu, P. Lu, and L.-W. Wang, Phys. Rev. B **95**, 035139 (2017), URL https://link.aps.org/doi/10.1103/PhysRevB.95.035139.

[69] G. Kang, Y. Kang, and S. Han, Phys. Rev. B **91**, 155141 (2015), URL https://link.aps.org/doi/10.1103/PhysRevB.91.155141.

[70] P. Liao and E. A. Carter, Phys. Chem. Chem. Phys. **13**, 15189 (2011), URL http://dx.doi.org/10.1039/C1CP20829B.

[71] G. Antonius, S. Poncé, P. Boulanger, M. Côté, and X. Gonze, Phys. Rev. Lett. **112**, 215501 (2014), URL https://link.aps.org/doi/10.1103/PhysRevLett.112.215501.

[72] F. Giustino, S. G. Louie, and M. L. Cohen, Phys. Rev. Lett. **105**, 265501 (2010), URL https://link.aps.org/doi/10.1103/PhysRevLett.105.265501.

[73] W. R. L. Lambrecht, C. Bhandari, and M. van Schilfgaarde, Phys. Rev. Materials **1**, 043802 (2017), URL https://link.aps.org/doi/10.1103/PhysRevMaterials.1.043802.

[74] S. Botti and M. A. L. Marques, Phys. Rev. Lett. **110**, 226404 (2013), URL https://link.aps.org/doi/10.1103/PhysRevLett.110.226404.

[75] J. Vidal, F. Trani, F. Bruneval, M. A. L. Marques, and S. Botti, Phys. Rev. Lett. **104**, 136401 (2010), URL https://link.aps.org/doi/10.1103/PhysRevLett.104.136401.

[76] F. Bechstedt, K. Seino, P. H. Hahn, and W. G. Schmidt, Phys. Rev. B **72**, 245114 (2005), URL https://link.aps.org/doi/10.1103/PhysRevB.72.245114.